IEICE TRANS. INF. & SYST., VOL.E91–D, NO.12 DECEMBER 2008

PAPER

Automatic Tortuosity-Based Retinopathy of Prematurity Screening System

Lassada SUKKAEW[†a)], ***Nonmember***, **Bunyarit UYYANONVARA**[†], ***Member***, **Stanislav S. MAKHANOV**[†], **Sarah BARMAN**[††], ***and*** **Pannet PANGPUTHIPONG**[†††], ***Nonmembers***

SUMMARY Retinopathy of Prematurity (ROP) is an infant disease characterized by increased dilation and tortuosity of the retinal blood vessels. Automatic tortuosity evaluation from retinal digital images is very useful to facilitate an ophthalmologist in the ROP screening and to prevent childhood blindness. This paper proposes a method to automatically classify the image into tortuous and non-tortuous. The process imitates expert ophthalmologists' screening by searching for clearly tortuous vessel segments. First, a skeleton of the retinal blood vessels is extracted from the original infant retinal image using a series of morphological operators. Next, we propose to partition the blood vessels recursively using an adaptive linear interpolation scheme. Finally, the tortuosity is calculated based on the curvature of the resulting vessel segments. The retinal images are then classified into two classes using segments characterized by the highest tortuosity. For an optimal set of training parameters the prediction is as high as 100%.

key words: *tortuosity, retinopathy of prematurity, segmentation*

1. Introduction

Retinopathy of Prematurity (ROP), previously known as retrolental fibroplasia, is a disease of the eye that affects premature infants. When a premature baby is born, the retinal blood vessels have not completed their development. In cases of patients with ROP, the blood vessels stop growing and new, abnormal blood vessels grow instead of the normal ones. The most severe complication of this disease is bilateral blindness in early childhood. ROP is characterized by an increase of tortuosity and abrupt changes in the growth of blood vessels near the optic disc. It has been estimated that more than 500 infants a year are blinded by retinopathy of prematurity in the U.S. alone [29].

The first step of computer aided detection of the ROP is finding the vessels in the input image. In this paper, mathematical morphology techniques are chosen because they are efficient and fast [1]. Morphological image processing is in particular useful in extracting image features whose shape is known a priori which is the case for the vasculature structures. Morphological processing is also resistant to noise [2]–[7].

Tortuosity evaluation is, however, still an open problem relevant to the clinical perception of the ophthalmologists. There exists a variety of methods to measure the tortuosity based on calculation of the ratio between the arc length and the chord length [8], [9]. Kylstra et al. [10] measures tortuosity using the relative length variation. His study includes relationships between tortuosity, diameter, and pressure that affect the change of the shape of artificial latex vessels. Kaupp et al. [11] proposed to measure the tortuosity by using the Fourier analysis. Capowski et al. [12] proposed a method of measuring tortuosity by using frequency analysis combined with a detection of changes in the size of the blood vessels. Dougherty and Varro [13] calculated the tortuosity using second derivatives along central axis of the blood vessels.

Five new integral estimates of tortuosity have been introduced by Smedby et al. [14]. Hart et al. [15] present another seven integral estimates of tortuosity based on the curvature of the vessels. Bullitt et al. [16] generalized Hart's estimates to 3D images obtained by means of the MRA for a better accuracy of the tortuosity calculation. Grisan et al. [17] proposed a new method based on partitioning of the blood vessels into segments using turning points, and calculating the tortuosity for each individual segment.

However, all the above estimates depend on the curve partition and may not always represent the tortuosity correctly. For example, a circle arc with a large radius is non tortuous although the ratio between arc length and chord length could be very large.

We propose a method to measure tortuosity of the vessels from retinal images using an adaptive linear interpolation procedure characterized by a certain choice of the maximum allowable interpolation error. The interpolation error controls the number of nodes and the choice of chords involved in the calculation of tortuosity. The interpolation procedure is combined with a tortuosity calculation for a single segment proposed in [17].

2. Proposed Method

This section consists of 5 chapters corresponding to the steps of our algorithm. Section 2.1 deals with vessel skeleton extraction. Section 2.2 describes how the vessels are partitioned into smaller segments using the maximum allowable interpolation error. Section 2.3 explains how a grid search for the best parameters for the partitioning is performed. Section 2.4 presents a general formula for tortuosity calculation. Finally, Sect. 2.5 deals with our classification

Manuscript received January 9, 2008.
Manuscript revised July 10, 2008.

[†]The authors are with Sirindhorn International Institute of Technology, Thammasat University, Thailand.
[††]The author is with Kingston University, United Kingdom.
[†††]The author is with Mettapracharak Hospital, Thailand.
a) E-mail: lassada@siit.tu.ac.th

DOI: 10.1093/ietisy/e91–d.12.2868

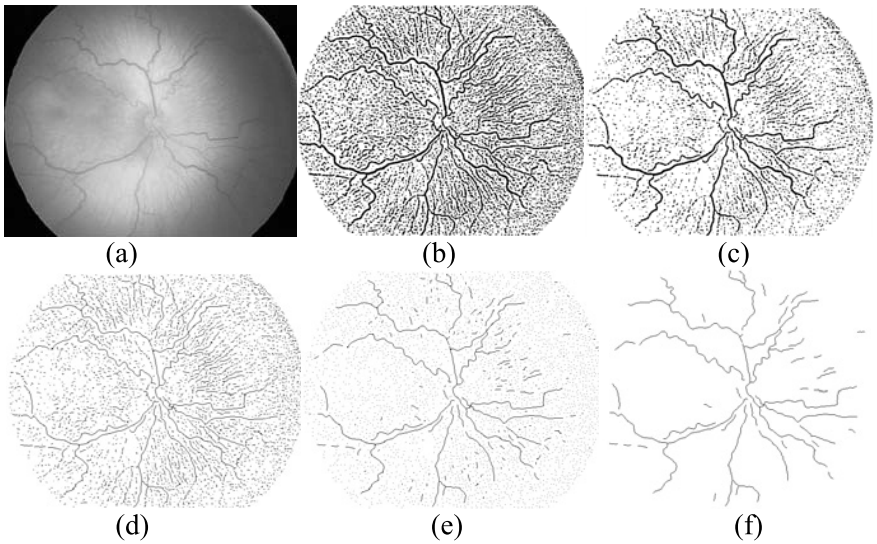

Fig. 1 (a) The original image, (b) edge detection, (c) Otsu threshold, (d) median axis skeleton, (e) pruning, (f) spurs removal.

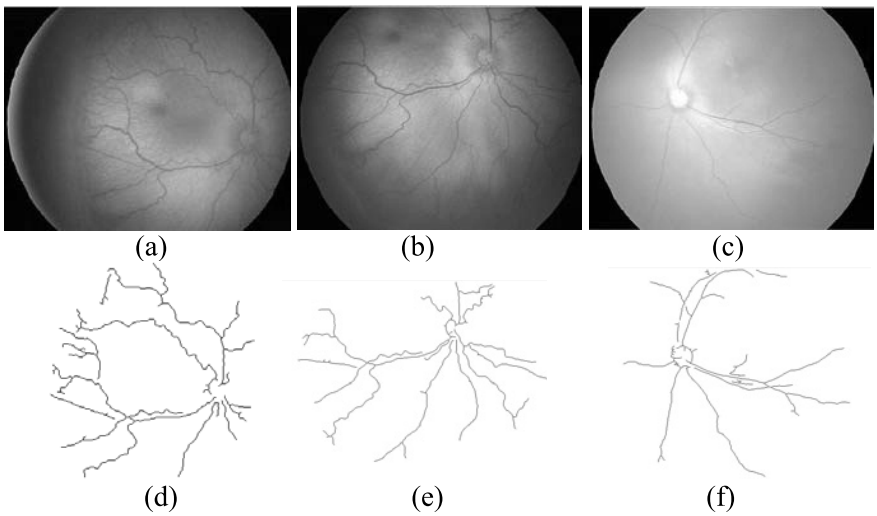

Fig. 2 (a) (b) and (c) the original images (d), (e) and (f) the detected vessels skeletons for (a), (b) and (c) respectively.

procedure.

2.1 Extraction of the Vessel Skeleton

Below is a short description of the extraction procedure (see details on [1]). The LOG filter [22] is applied to extract the edges from the original, possibly low-contrast retinal image. The results are then thresholded using an optimal threshold selected by the Otsu algorithm [23]. The edge image is then skeletonised using the medial axis skeletonisation [24]. It is well known that skeletonisation often produces short extraneous spurs. These noises which may occur from the previous step are suppressed by a pruning process [25]. The result is finalized by removing small isolated clusters (islands) of noise using morphological opening. The island removal algorithm employs erosion followed by dilation [26]–[28].

The algorithm is illustrated in Figs. 1 and 2. The output image contains centreline pixels associated with the extracted blood vessels (Fig. 1 (f) and Fig. 2 (d), (e) and (f)).

2.2 Recursive Vessel Partitioning

The curvature of the blood vessel is the most important parameter that characterizes the tortuosity. However, a straightforward integration of the curvature along the vessel is not the best option. This is because on average the curvature might not be very large, but it can be large along a certain part of the vessel. Therefore, in this paper, by imitating expert ophthalmologists, we understand the tortuosity as high curvature of the blood vessel along a certain segment. However, we do not define the size of this segment in advance.

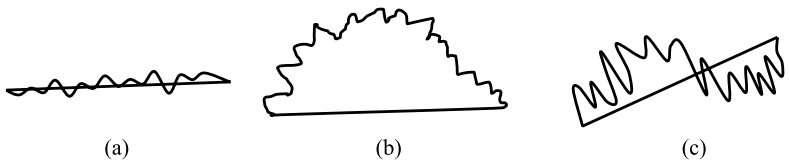

Fig. 3 Evaluation of the curvature by splitting the curve into segments (a) acceptable segment with small deviation from the straight line (b) unacceptable segments (c) acceptable segment with higher deviation from the straight line.

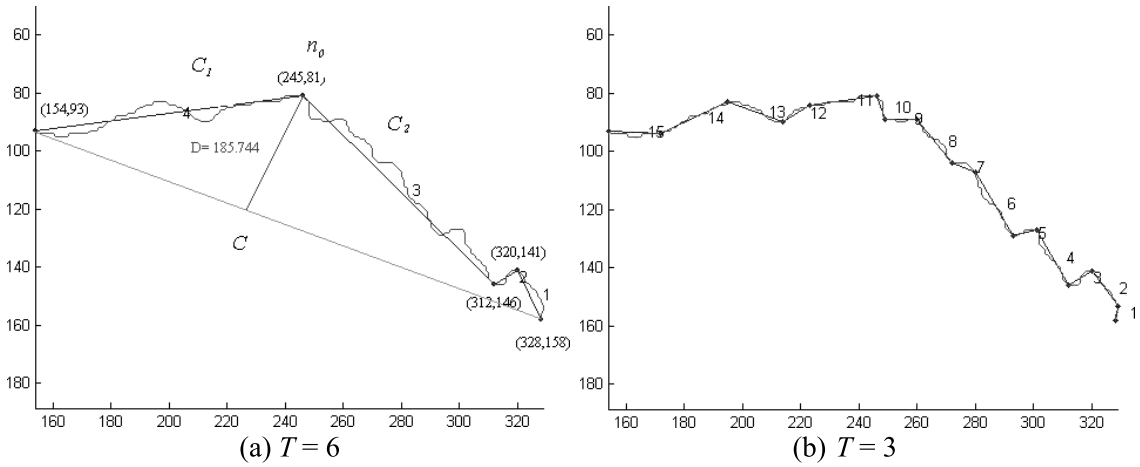

Fig. 4 (a) First step of segmentation, (b) final partition.

In [10] the curve is partitioned into segments using the so called turn points that are the points where the curvature changes the sign. As opposed to that, our method is based on finding a set of chords having approximately the same deviation from the original curve. We believe that this procedure is close to the way the humans evaluate the curvature. We split the blood vessels into segments using a procedure which evaluates the maximum deviation of the curve from the straight lines. The proposed partition is based on the intuitive understanding that the evaluation of the tortuosity by humans is based on splitting the curve into segments having on average the same deviation from the corresponding chord and evaluating the ratio between the length of the chord and the length of the curve. The chord should not be too close to or too far from the curves (see Fig. 3).

Mathematically it means that each segment S from blood vessel V is defined using a piecewise linear interpolating function constructed with an adaptive choice of nodes. The nodes are selected using bisection. The first segment is represented by the entire blood vessel, that is $S = B$. It is approximated by a chord C using the two boundary nodes (see Fig. 3 (a)). The next node is obtained as follows

$$n_0 = \arg\max |C - S|.$$

In words, the first node is inserted at the point of the maximum allowable interpolation error of segment S from chord C. Next, S is split by node n_0 into two curves S_1 and S_2. The next node n_1 is obtained using the corresponding chords C_1 and C_2.

$$n_1 = \arg\max\{\max |C_1 - S_1|, \max |C_2 - S_2|\}.$$

The process runs recursively and it stops when $\max |C_i - S_i| < T$, $\forall i$, where T is the prescribed threshold (maximum interpolation error). Figure 4 illustrates the algorithm, (a) shows the first step of segmentation and (b) the final partition. Figure 5 displays the partitioned vessels from two different images.

2.3 Grid Search for Maximum Allowable Interpolation Error

We find the best maximum allowable interpolation error by a grid search for $T = 6$, 10, 15 and 20. In order to train the classifier we use ground truth expert ophthalmologists with Mettapracharuk Hospital in Thailand. We calculate the tortuosity for every segment in the image separately and select five most tortuous segments as features for classification. The comparison process is explained in detail in Sect. 2.4. The result of the training is T that gives the highest accuracy rate. Two examples of resulting vessel partitioning with different maximum allowable interpolation errors are shown in Figs. 6 and 7.

2.4 Tortuosity Calculation

To calculate the tortuosity we use a formula proposed by Gaisan [17]

$$\tau(C) = \frac{n-1}{length(C)} \sum_{i=1}^{n} \left[\frac{length(S_i)}{length(C_i)} - 1 \right],$$

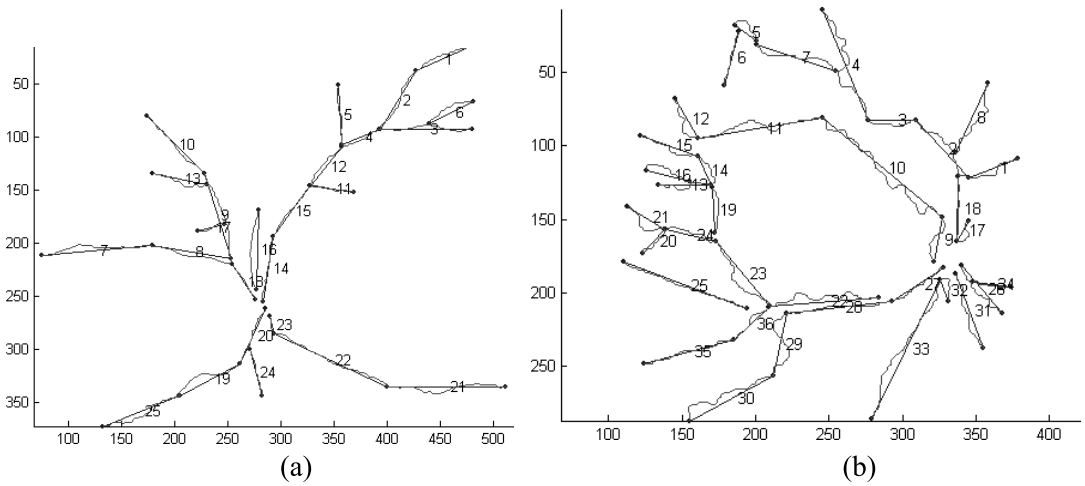

Fig. 5 (a) and (b) vessel partitioning from different images.

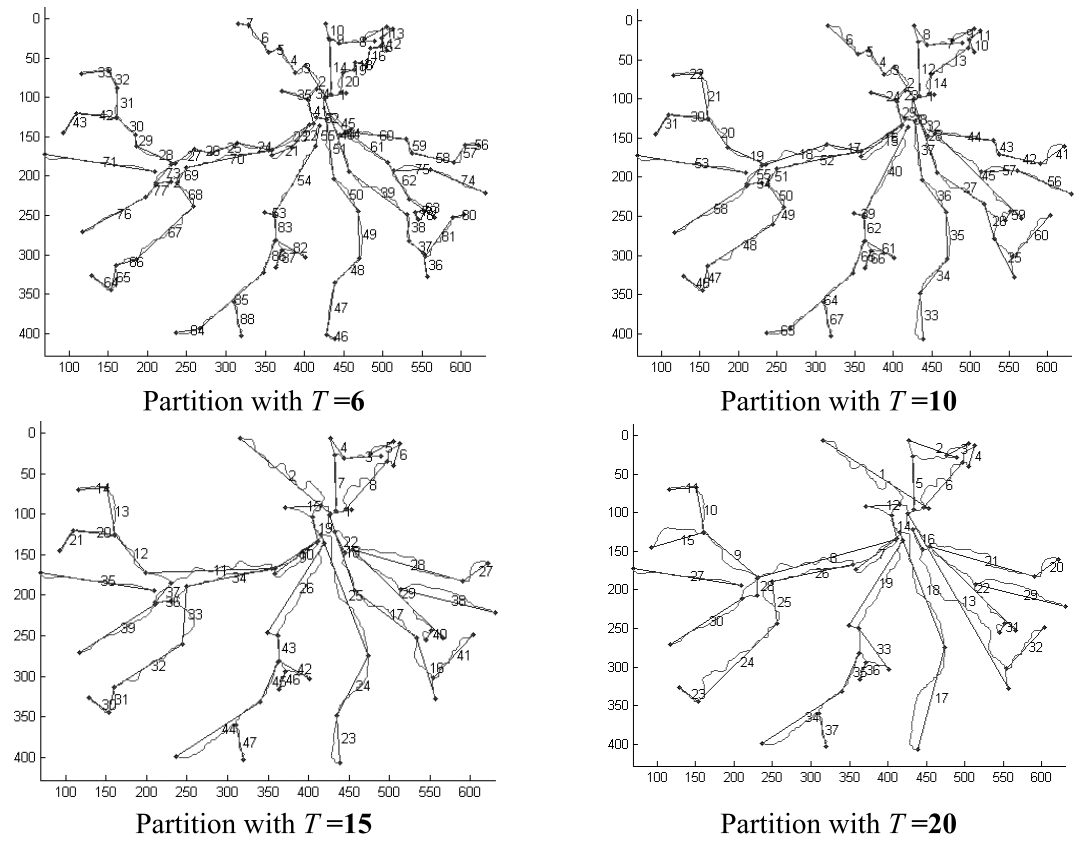

Fig. 6 Partitioning with varying T.

where i is the segment number and n the total number the segments. The tortuosity measure has a dimension of 1/length and thus is interpreted as the tortuosity density.

2.5 Classification

In order to classify the retinal images into two classes of high risk and low risk of having ROP, an expert ophthalmologist looks for tortuous sections of vessels on a retina. If certain segments are found to be tortuous, the expert says that this child has a high risk developing ROP.

In this paper we imitate this process by selecting several most tortuous segments as a set of the classification features. In order to select tortuous images the following condition is used.

$$m - \alpha\sigma > \tau_t,$$

where m is the average tortuosity of the selected images, σ

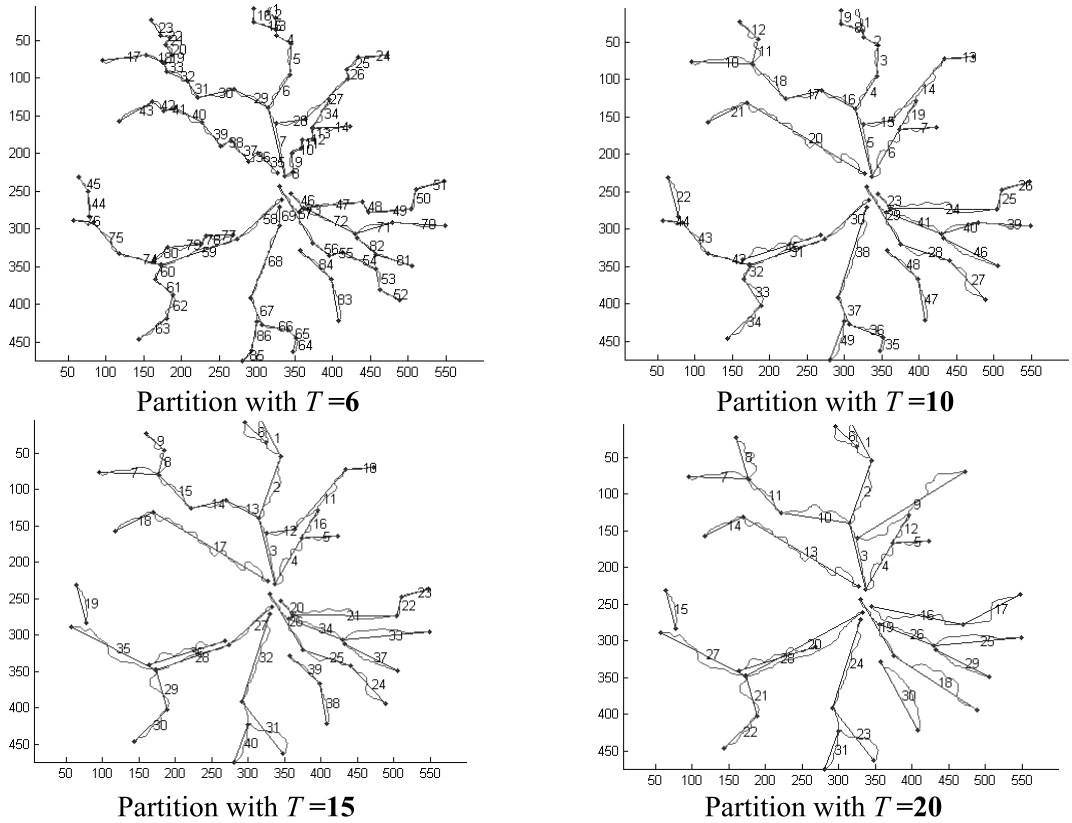

Fig. 7 Partitioning with varying T.

Table 1 Classification with $T = 10$.

Image No	1	2	3	4	5	Means	STD	$m-\alpha\sigma$	Ground Truth	Prediction
1	0.894	0.659	0.422	0.381	0.322	0.536	0.238	0.298	Tortuous	Tortuous
2	0.418	0.389	0.337	0.307	0.288	0.348	0.055	0.293	Tortuous	Tortuous
3	0.341	0.301	0.289	0.281	0.279	0.298	0.025	0.273	Tortuous	Tortuous
4	0.485	0.340	0.325	0.307	0.275	0.346	0.081	0.265	Normal	Tortuous
5	0.467	0.411	0.393	0.349	0.166	0.357	0.115	0.242	Normal	Normal
6	0.325	0.300	0.281	0.281	0.177	0.273	0.057	0.216	Normal	Normal
7	0.306	0.253	0.217	0.214	0.196	0.237	0.044	0.194	Normal	Normal
8	0.303	0.275	0.244	0.184	0.183	0.238	0.054	0.184	Normal	Normal
9	1.145	0.872	0.476	0.270	0.191	0.591	0.407	0.184	Normal	Normal
10	0.275	0.259	0.240	0.183	0.180	0.227	0.044	0.183	Normal	Normal

is the standard deviation, α is the calibration parameter, and τ_t the threshold. The above estimate selects images characterised by a large average tortuosity and a small standard deviation.

3. Model Verification

One hundred images (480×460 pixels, 24 bits per pixel, with no compression) were used to test the proposed method. All the images were sent to two expert ophthalmologists for the visual classification. The ophthalmologists analyzed each image as a whole and classified that image as tortuous or non-tortuous based solely on their expertise. If the results from the both experts agreed, they would be used as a ground truth in the training and the testing phase. The usual ratio 3/7 was used for the testing and training. The training produced $\tau' = 0.25$, $\alpha = 1$ and $T = 10$.

Consider now results of the test classification. Tables 1 and 2 display the case $T = 10$ and T 15 respectively.

Tables 1 and 2 display characteristics of ten images with the highest $m - \alpha\sigma$. We number the images in the first Table from 1 to 10 and show the corresponding images in Table 2 with the same numbers. If a new image appears, we assign to it a next consecutive number.

The experiment with 100 images reveals the best T ranging from $T = 10$ to $T = 15$. For these values the prediction accuracy of 100% is achieved.

4. Conclusion

We present and analyze a simple technique for classification of the retinal images into tortuous and non tortuous based

Table 2 Classification with $T = 15$.

Image No	1	2	3	4	5	Means	STD	$m-\alpha\sigma$	Ground Truth	Prediction
1	0.894	0.659	0.490	0.431	0.373	0.570	0.210	0.359	Tortuous	Tortuous
2	0.418	0.389	0.337	0.333	0.323	0.360	0.041	0.319	Tortuous	Tortuous
3	0.441	0.341	0.289	0.281	0.279	0.326	0.069	0.257	Tortuous	Tortuous
6	0.325	0.283	0.281	0.281	0.203	0.275	0.044	0.230	Normal	Normal
4	0.908	0.485	0.350	0.325	0.318	0.477	0.250	0.227	Normal	Normal
8	0.339	0.323	0.303	0.275	0.183	0.285	0.062	0.223	Normal	Normal
11	0.661	0.469	0.301	0.259	0.217	0.381	0.183	0.198	Normal	Normal
12	0.467	0.346	0.345	0.265	0.144	0.314	0.119	0.194	Normal	Normal
13	0.560	0.497	0.270	0.223	0.213	0.353	0.163	0.189	Normal	Normal
14	0.254	0.233	0.219	0.207	0.174	0.217	0.030	0.187	Normal	Normal

on adaptive vessel partitioning and a grid search for the best maximum allowable interpolation error.

We also propose a new threshold based on a linear combination of the standard deviation and the mean of the selected most tortuous segments of the vessel network.

The method imitates evaluation of the tortuosity performed by humans based on splitting of the vessels into segments characterized by a certain degree of the deviation from imaginary straight lines.

The numerical experiments show the efficiency and robustness of the proposed method as applied to 100 medical images of the retina. The best set of parameters produces 100% classification rate.

Acknowledgement

The authors are grateful to the Director of Mettapracharuk Hospital in Nakorn Pathom, Thailand. We also would like to thank MD Maytinee Sirimaharaj for her very helpful support on the medical side of this paper. Finally, we wish to thank Alistair Fielder and Ken Cocker with City University of the UK, for providing the ROP images for this research.

References

[1] L. Sukkaew, B. Uyyanonvara, S. Barman, A. Fielder, and K. Cocker, "Automatic extraction of the structure of the retinal blood vessel network of premature infants," J. Medical Association of Thailand, vol.90, no.9, pp.1780–1792, 2007.

[2] F. Zana and J.C. Klein, "Robust segmentation of vessels from retinal angiography," Proc. International Conference on Digital Signal Processing, pp.1087–1091, Santorini, Greece, 1997.

[3] F. Zana and J.C. Klein, "A multimodal registration algorithm of eye fundus images using vessels detection and Hough transform," IEEE Trans. Med. Imaging, vol.18, pp.419–427, 1999.

[4] F. Zana and J.C. Klein, "Segmentation of vessel-like patterns using mathematical morphology and curvature evaluation," IEEE Trans. Image Process., vol.10, pp.1010–1019, July 2001.

[5] M. Donizelli, Region-oriented segmentation of vascular structures from DSA images using mathematical morphology and binary region growing, Bildverarbeitung für die Medizin, 1998.

[6] S. Eiho and Y. Qian, "Detection of coronary artery tree using morphological operator," IEEE Computers in Cardiology, vol.24, pp.525–528, 1997.

[7] B.D. Thackray and A.C. Nelson, "Semi-automatic segmentation of vascular network images using a rotating structuring element (rose) with mathematical morphology and dual features thresholding," IEEE Trans. Med. Imaging, vol.12, pp.385–392, Sept. 1993.

[8] W. Lotmar, A. Freiburghaus, and D. Bracher, "Measurement of vessel tortuosity on fundus photographs," Graefe's Archive for Clinical and Experimental Ophthalmology, vol.211, pp.49–57, 1979.

[9] D. Bracher, "Changes in peripapillary tortuosity of the central retinal arteries in newborns," Graefe's Archive for Clinical and Experimental Ophthalmology, vol.218, pp.211–217, 1986.

[10] J.A. Kylstra, T. Wierzbicki, M.L. Wolbarsht, M.B. Landers, III, and E. Stefansson, "The relation ship between retinal vessel tortuosity, diameter and transmural pressure," Graefe's Archive for Clinical and Experimental Ophthalmology, vol.224, pp.477–480, 1986.

[11] A. Kaupp, H. Toonen, S. Wolf, K. Schulte, R. Effert, D. Meyer-Ebrecht, and M. Reim, "Automatic evaluation of retinal vessel width and tortuosity in digital fluorescein angiograms," Investigative Ophthalmology & Visual Science, vol.32, p.952, 1991.

[12] J.J. Capowski, J.A. Kylstra, and S.F. Freedman, "A numeric index based on spatial-frequency for the tortuosity of retinal-vessels and its application to plus disease in retinopathy of prematurity," Retina, vol.15, no.6, pp.490–500, 1995.

[13] G. Dougherty and J. Varro, "A quantitative index for the measurement of the tortuosity of blood vessels," Medical Engineering & Physics, vol.22, pp.567–574, 2000.

[14] O. Smedby, N. Hogman, S. Nilsson, U. Erikson, A.G. Olsson, and G. Walldius, "Two-dimensional tortuosity of the superficial femoral artery in early atherosclerosis," J. Vascular Research, vol.30, pp.181–191, 1993.

[15] W. Hart, M. Golbaum, B. Cote, P. Kube, and M. Nelson, "Measurement and classification of retinal vascular tortuosity," Int. J. Medical Informatics, vol.53, pp.239–252, 1999.

[16] E. Bullitt, G. Gerig, S. Pizer, W. Lin, and S. Aylward, "Measuring tortuosity of the intracerebral vasculature from MRA images," IEEE Trans. Med. Imaging, vol.22, no.9, pp.1163–1171, 2003.

[17] E. Gaisan, M. Foracchia, and A. Ruggeri, "A novel method for the automatic evaluation of retinal vessel tortuosity," Proc. 25th Annual International Conference of the IEEE Engineering in Medicine and Biology, Cancun, Mexico, Sept. 2003.

[18] R. Duda, P. Hart, and D. Stork, Pattern Classification, 2nd ed., John Wiley & Sons, New York, 2001.

[19] J. Staal, M.D. Abramoff, M. Niemeijer, M.A. Viergever, and B. van Ginneken, "Ridge-based vessel segmentation in color images for the retina," IEEE Trans. Med. Imaging, vol.23, no.4, pp.501–509, 2004.

[20] M. Niemeijer, J. Staal, B. van Ginneken, M. Long, and M.D. Abramoff, "Comparative study of retinal vessel segmentation methods on a new publicly available database," Proc. SPIE Medical Imaging, vol.5370, pp.648–656, 2004.

[21] N. Salem and A. Nandi, "Segmentation of retinal blood vessels using scale-space features and K-nearest neighbour classifier," ICASSP2006, pp.1001–1004, 2006.

[22] L. Sukkaew and B. Uyyanonvara, "Automatic skeletonized structure detection of premature infant's low-contrast retinal blood vessel network," Proc. InTech Conference, pp.3882–3892, 2005.

[23] N. Otsu, "A threshold selection method from gray-level histograms," IEEE Trans. Syst. Man Cybern., vol.9, no.1, pp.62–66, 1979.

[24] R. Haralick and L. Shapiro, Computer and Robot Vision, vol.I, pp.233, 348–349, Addison-Wesley Publishing Company, 1992.
[25] R. Gonzalez and R. Woods, Digital Image Processing, pp.540–543, Addison-Wesley Publishing Company, 1993.
[26] R. Jain, R. Kasturi, and B.B. Schunck, Machine Vision, McGraw Hill, 1995.
[27] S.E. Umbaugh, Computer Vision and Machine Processing, PHPTR, 1998.
[28] J. Serra, Image Analysis and Mathematical Morphology, Academic, London, U.K. 1982.
[29] http://www.nfb.org/images/nfb/Publications/fr/fr5/Issue2/f0502tc.html
The National Federation of the Blind Magazine for Parents and Teachers of Blind Children, vol.5, no.2, 1986.

Lassada Sukkaew received the B.B.A degree from Rajamangala University of Technology Thanyaburi, Thailand in 1998, B.Tech degree in business information technology from Sukhaothai Thammathirat University Thailand in 2003, and M.Sc. in computer and information technology from King Mongkut's University of Technology Thonburi, Thailand in 2001. She is currently a Ph.D. student with the School of Information and Computer Technology at Sirindhorn International Institute of Technology, Thammasat University of Thailand. She is also an instructor with Faculty of Business Administration of Rajamangala University of Technology Srivijaya. Her research interests are medical image processing and image analysis.

Bunyarit Uyyanonvara recieved his Ph.D. in Medical Image Analysis from King's College, London in 2000 and a B.Sc. of Science (1st Class Honours) from Prince of Songkhla University, Thailand. He is now an assistant professor at Sirindhorn International Institute of Technology, Thammasat University, Thailand.

Stanislav S. Makhanov recieved the M.Sc. in Applied Mathematics from Moscow State University in 1981 and the Dr.Sc. from Computing Center of the Russian Academy of Science in 1988. He is currently Associate Professor with Sirindhorn International Institute of Technology of Thailand (SIIT). He is teaching courses in Applied Mathematics and Computer Science. Dr. Makhanov has published about 100 research papers and conference proceedings in numerical methods for robotics, image processing and CFD.

Sarah Barman received her Ph.D. in Optical Physics from King's College, London in 1996. She obtained an M.Sc. in Applied Optics from Imperial College London and a B.Sc. in Physics from Essex University. She is now a Senior Lecturer at the Digital Imaging Research Centre in the Faculty of Computing, Information Systems and Mathematics at Kingston University.

Pannet Pangputhipong was born on September 28, 1959 in Bangkok, Thailand. He finished medical degree in 1982 at King Chulalongkorn University and Board of Ophthalmology in 1988 at Rajvithee hospital, Ministry of Public Health. He is now working as the Director of Mettapracharak Hospital and Center for Ophthalmology.